

Generating Fair Universal Representations using Adversarial Models

Peter Kairouz*, Jiachun Liao*, Chong Huang, Maunil Vyas, Monica Welfert, Lalitha Sankar

Abstract—We present a data-driven framework for learning *fair universal representations* (FUR) that guarantee statistical fairness for any learning task that may not be known *a priori*. Our framework leverages recent advances in adversarial learning to allow a data holder to learn representations in which a set of sensitive attributes are decoupled from the rest of the dataset. We formulate this as a constrained minimax game between an encoder and an adversary where the constraint ensures a measure of usefulness (utility) of the representation. The resulting problem is that of censoring, i.e., finding a representation that is least informative about the sensitive attributes given a utility constraint. For appropriately chosen adversarial loss functions, our censoring framework precisely clarifies the optimal adversarial strategy against strong information-theoretic adversaries; it also achieves the fairness measure of demographic parity for the resulting constrained representations. We evaluate the performance of our proposed framework on both synthetic and publicly available datasets. For these datasets, we use two tradeoff measures: censoring vs. representation fidelity and fairness vs. utility for downstream tasks, to amply demonstrate that multiple sensitive features can be effectively censored even as the resulting fair representations ensure accuracy for multiple downstream tasks.

Index Terms—Fair universal representations, algorithmic fairness, generative adversarial networks, minimax games.

I. INTRODUCTION

The use of data-driven machine learning (ML) has recently seen unprecedented success in a variety of automated decision-making systems including facial recognition, natural language processing, mortgage lending, and even parole prediction. The success of these approaches hinges on the availability of large datasets that often include sensitive personal information. It has been shown that models learned from such datasets can inherit societal bias and discrimination patterns [1], [2] and learn sensitive features even when they are not explicitly used during training [3]. Concerns about the fairness, bias, and privacy of learning algorithms have led to a growing body of research focused on both defining meaningful fairness measures and designing algorithms with such guarantees.

A key challenge in algorithmic fairness is the quantification of disparate treatment and impact – legal notions developed to ensure that societal decisions neither hinder nor discriminate against specific groups. Addressing this has broadly lead to two classes of measures: (i) group fairness measures which require similar outcomes for all groups [4]; (ii) individual fairness measures which require treating similar individuals similarly [5]. Approaches combining both fairness requirements have also been considered [6], [7]. In the context of supervised

learning of intended tasks (our setting here), two key group fairness measures have emerged [8]: (i) demographic parity (DemP) which requires predicted outcomes to be independent of the sensitive features, and (ii) equalized odds (EO) wherein such an independence holds only when conditioned on the true outcome. The EO measure was introduced to ensure accurate predictions within groups, a limitation of DemP [9].

Three distinct approaches have been considered to enforce fairness in learning: in-processing, pre-processing, and post-processing. In-processing approaches are most commonly used in the supervised setting where the learning objective is known (e.g., [5], [10]); the resulting trained model guarantees fairness for the specific objective. Pre-processing generally produces fair representations of data tuned for a chosen learning objective [11], [12] while post-processing provides fairness by properly altering decision outputs [13], [14].

Recently, *censoring* has emerged as a compelling pre-processing approach wherein protected features (e.g., race, gender, and their correlates) are actively decorrelated from the rest of the data to explicitly limit their effect on decisions. Censoring is inspired by information-theoretic privacy methods to limit leakage of sensitive features [3], [15]–[18] and can be achieved in practice using generative adversarial networks (GANs) [19], [20]. Thus far, censoring for fairness has largely focused on learning fair predictors [10]–[12].

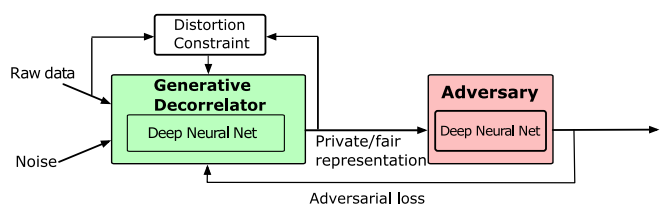


Figure 1: Generative adversarial model for censoring and fairness.

Our Contributions: Taking a preprocessing approach, the main contribution of this work is to use censoring to generate fair representations that are *universal*. These are representations from which the sensitive features have been actively decoupled and can be universally used for a variety of *a priori* unknown learning tasks. We show that such fair universal representations (FURs) can assure DemP group fairness for all downstream predictions (from the data processing inequality). We now detail our contributions:

- We present a framework for learning FURs as a minimax game between an encoder¹ and an adversary, where the

¹referred to interchangeably throughout the paper as fair encoder or generator or decorrelator

*: equal contribution

This work is supported in part by the National Science Foundation under grants CCF-1350914, CIF-1815361, CIF-1901243, SaTC-2031799, and CIF-2007688.

encoder *generates a noisy representation* of the original data to thwart an adversary that actively tries to infer the sensitive features (see Fig. 1). In contrast to adversarial methods that generate intermediate representations intended to assure a specific fair prediction (e.g., [11]), we focus on generating FURs, and to this end, define demographic parity for FRs. We use censoring (the sensitive features) to achieve DemP FRs and provide information-theoretic assurances on both.

- The FUR minimax game is zero-sum, i.e., the adversary and the encoder maximize and minimize, respectively, the same objective, namely, the average loss in inferring the sensitive features from the representation. To avoid the trivial solution of generating independent noise and ensure the universality of the created representations, we introduce a *hard* constraint on the representation’s fidelity. Here again, our approach is in contrast to fair predictors where the classifier’s performance is included in the objective via a *fixed* Lagrange parameter. Hard constraints further increase the complexity of training adversarial models. A key contribution of this work is in leveraging Lagrange penalty methods [21] effectively in a GAN-setting. In fact, recently TensorFlow updated its package to allow enforcing hard constraints [22] using a similar approach.
- The FUR minimax game we consider can capture a range of adversarial actions through the choice of loss functions. For any encoder, we determine the information-theoretic optimal adversarial action for a large class of loss functions that capture inferential behavior, including the recently introduced tunable class, α -loss for $\alpha \in (0, \infty)$ [23]. For synthetic Gaussian data, this allows us to evaluate the performance of the empirical FUR framework (using neural networks) under log-loss ($\alpha = 1$) to the game-theoretic optimal under the strongest MAP (maximum *a posteriori*) adversary ($\alpha = \infty$). While provable guarantees for fair representations has been studied for cross-entropy loss and squared loss [24], our FUR framework provides such guarantees for a large class of adversaries and distortion functions.
- We show that, under α -loss, the FUR minimax game simplifies to minimizing the order α -Arimoto mutual information (MI) subject to a constraint. Thus, our approach provides an alternative to ML practitioners interested in optimizing empirical information-theoretic measures (e.g., Shannon MI for $\alpha = 1$, i.e., log-loss). Instead of using variational techniques (i.e., optimizing lower/upper bounds on the objective function) [25], we show that one can do so using a minimax formulation with an appropriate loss function. On the fairness front, for α -loss as the adversarial loss, we demonstrate how minimizing Arimoto MI, for all α can serve as a strong proxy for demographic parity.
- Finally, we illustrate the utility of FURs using: (i) multi-dimensional synthetic Gaussian data; and (ii) multiple publicly datasets used for censoring and fairness including the UCI Adult, UTKFace, GENKI, and HAR datasets. For relevant datasets, our visual results demonstrate our success in creating high quality representations that increasingly erase the sensitive attributes with decreasing fidelity requirements. In contrast to state-of-the-art [10]–[12], our theoretical framework and our experiments consider non-

binary sensitive attributes as well as multiple downstream tasks. Our experimental results show that one can still learn high accuracy DemP (and even EO) fair classifiers from DemP FURs. In particular, the UCI dataset that is often used in fair ML analyses showcases the advantage of our approach relative to related approaches (see, for example, [12], [10], [11], [26]). Our results also straddle a wide range of values for the chosen fairness measure (DemP) and include perfect fairness, in contrast to the above works.

The remainder of our paper is organized as follows. We formally define censored and fair representations in Section II. In Section III, we formalize our FUR model and highlight the theoretical guarantees of this approach. In Section IV, we present theoretical results for datasets modeled as multi-dimensional Gaussian mixtures. Finally, we showcase the performance of the FUR framework on the UCI Adult and UTKFace datasets in Section V. All proofs and algorithms are relegated to the appendix. Finally, details on architecture for all datasets as well as the results for the GENKI and HAR datasets are in the accompanying supplementary material.

II. PRELIMINARIES

Consider a dataset \mathcal{D} with n entries where each entry is a random tuple $(S, X, Y) \in \mathcal{S} \times \mathcal{X} \times \mathcal{Y}$ where S , X , and Y are sensitive, non-sensitive, and target (non-sensitive) features, respectively, and $\hat{Y} \in \mathcal{Y}$ is a predictor of Y . Note that S and Y can be a collection of features or labels (e.g., S can be gender, race, or sexual orientation, while Y could be age, facial expression, etc.); for ease of writing, we use the term variable to denote both single and multiple features/labels. Instances of X , S , and Y are denoted by x , s and y , respectively. The entries (X, S, Y) of \mathcal{D} are independent and identically distributed (i.i.d.) according to $P(X, S, Y)$.

Recent results on algorithmic fairness guarantee that, for a specific target Y , the prediction of a machine learning model is accurate with respect to (*w.r.t.*) Y but unbiased *w.r.t.* the sensitive S . While more than two dozen measures for fairness have been proposed, two oft-used fairness measures are demographic parity and equalized odds (and variants thereof). Demographic parity (DemP) ensures complete independence between the prediction of the target \hat{Y} and the sensitive S ; this notion of fairness favors utility the least, especially when Y and S are correlated [8]. Equalized odds (EO) enforces this independence conditioned on Y , thereby ensuring equal rates for true and false positives (when Y is binary) for all demographics. We now define DemP and EO formally (for binary S and Y as originally introduced). These definitions can be generalized to the non-binary setting and we do so in the sequel for fair representations.

Definition II.1 ([8]). A predictor $f(S, X) = \hat{Y}$ satisfies

- *demographic parity (DemP) w.r.t. S , if $\hat{Y} \perp S$, i.e.,*

$$\Pr(\hat{Y} = 1|S = 1) = \Pr(\hat{Y} = 1|S = 0) \quad (1)$$

- *equalized odds (EO) w.r.t. (S, Y) , if $\hat{Y} \perp S|Y$, for $y \in \{0, 1\}$:*

$$\Pr(\hat{Y} = 1|S = 1, Y = y) = \Pr(\hat{Y} = 1|S = 0, Y = y). \quad (2)$$

We now define censoring and fairness for representations. Our censoring definition clarifies the representation that best limits an adversary from inferring S . We then define DemP for FRs; we combine the two definitions to show how and when adversarial learning can help ensure demographic parity.

Definition II.2 (Censored Representations). *A representation X_r of X is censored w.r.t. the sensitive features S against a learning adversary $h(\cdot)$, whose performance is evaluated via a loss function $\ell(h(X_r), S)$, if for an optimal adversarial strategy $h^* = \operatorname{argmin}_h \mathbb{E}[\ell(h(X_r), S)]$,*

$$\mathbb{E}[\ell(h^*(g(\cdot)), S)] \leq \mathbb{E}[\ell(h^*(X_r), S)], \quad (3)$$

where $g(\cdot)$ is any (randomized) function of X (or (X, S)) and the expectation is over h , g , X , and S .

The above definition suggests that the best censored representation X_r is the least informative about S to an adversary whose inferential action is captured by a loss function $\ell(\cdot, \cdot)$, i.e., the average loss is the worst for X_r than for any other arbitrary function $g(\cdot)$. While the comparison in (3) is w.r.t. the best $h^*(X_r)$ for X_r , choosing the optimal $h(\cdot)$ for any $g(\cdot)$ will only serve as a lower bound to the left side of (3).

We now define DemP for representations; we then prove that a demographically fair representation X_r guarantees that any downstream algorithm using X_r satisfies DemP w.r.t. S .

Definition II.3 (Demographically Fair Representations). *For $(X, S) \in \mathcal{X} \times \mathcal{S}$, a representation $X_r = g(X, S) \in \mathcal{X}_r$ satisfies demographic parity w.r.t. S if for any $x_r \in \mathcal{X}_r$ and $s, s' \in \mathcal{S}$*

$$\Pr(X_r = x_r | S = s) = \Pr(X_r = x_r | S = s') \quad (4)$$

where $g : \mathcal{X} \times \mathcal{S} \rightarrow \mathcal{X}_r$ is any (possibly randomized) function.

Theorem 1 (Fair Learning via Fair Representation). *If $X_r = g(X, S)$ satisfies demographic parity w.r.t. S , then any algorithm $f : \mathcal{X}_r \rightarrow \mathcal{Y}$ satisfies demographic parity w.r.t. S .*

The proof of Theorem 1 follows from the data-processing inequality of mutual information as detailed in Appendix A.

Remark 1. *Note that equalized odds in Def. II.1 explicitly involves a downstream task, and therefore, the design of an EO fair X_r needs to include a predictor explicitly. In contrast to the FUR setting considered here, such targeted representations and the ensuing fair predictors provide guarantees only for specific target Y . In this limited context, however, one can still define an X_r as ensuring EO w.r.t. to (S, Y) if $\dot{Y}(X_r) \perp S | Y$.*

One simple approach to obtain a fair/censored representation X_r is by choosing $X_r = N$ where $N \perp (X, S)$. However, such an X_r has no utility (quantified, for example, via downstream task accuracy). The design of X_r has to ensure utility, and thus, there is a tradeoff between guaranteeing fairness/censoring and assuring a desired level of utility. We now quantify such tradeoffs using FUR framework.

III. FURs VIA GENERATIVE ADVERSARIAL MODELS

Formally, the FUR model consists of two components, an encoder and an adversary, as shown in Fig. 1. The goal of the encoder $g : \mathcal{X} \times \mathcal{S} \rightarrow \mathcal{X}_r$ is to actively eliminate the

dependence between S and X while that of the adversary $h : \mathcal{X}_r \rightarrow \mathcal{S}$ is to infer S . In general, $g(X, S)$ is a randomized mapping that outputs a representation $X_r = g(X, S)$. Note that S may not always be available to the curator; however, it will always affect the design of g via the adversarial training process. For brevity, we henceforth write $g(\cdot)$ to include both possibilities (just X or (X, S) as inputs). On the other hand, the role of the adversary is captured via $h(X_r)$, which is the adversarial decision rule in inferring the sensitive variable S as $\hat{S} = h(X_r = g(\cdot))$ from the representation $g(\cdot)$. In general, the hypothesis h can be a *hard decision rule* under which $h(g(\cdot))$ is a direct estimate of S or a *soft decision rule* under which $h(g(\cdot)) = P_h(\cdot | g(\cdot))$ is a distribution over \mathcal{S} .

To quantify the adversary's performance, we use a loss function $\ell(h(g(X = x, S = s)), S = s)$ defined for every pair (x, s) . Thus, the adversary's expected loss w.r.t. X and S is $L(h, g) \triangleq \mathbb{E}[\ell(h(g(\cdot)), S)]$, where the expectation is taken over $P(X, S)$ and the randomness in g and h . To ensure utility, we introduce a constraint on the fidelity of X_r via a distortion function $d(x_r, x)$, which measures the goodness of $X_r = x_r$ w.r.t. $X = x$. Ensuring statistical utility, in turn, requires constraining the average distortion $\mathbb{E}[d(g(\cdot), X)]$, where the expectation is taken over $P(X, S)$ and the randomness in g .

A. FUR: Framework and Theoretical Results

To publish a fair representation X_r , the data curator wishes to learn an encoder g that guarantees censoring (i.e., it is difficult for the adversary to learn S from X_r), and therefore, fair X_r under DemP, as well as utility (g guarantees bounded distortion of X). In contrast, for a fixed g , the adversary would like to find a (potentially randomized) function h that minimizes its expected loss, or equivalently maximizes the negative expected loss. This leads to a constrained minimax game between the encoder and the adversary given by

$$\min_{g(\cdot)} \max_{h(\cdot)} -\mathbb{E}[\ell(h(g(\cdot)); S)], \text{ s.t. } \mathbb{E}[d(g(\cdot), X)] \leq D. \quad (5)$$

where $D \geq 0$ determines the distortion constraint on X_r . The optimization in (5) highlights that the input to g depends on whether the curator has access to both (X, S) or just X . Having access to both (X, S) in general will yield a better decorrelator (e.g., see Section V-A for the UCI dataset). Finally, without the constraint in (5), the optimal $X_r = g(\cdot) \perp S$. One can approximate this in practice via arbitrarily large distortions leading to the following Proposition.

Proposition 1. *For sufficiently large distortion bound D , (5) yields a universal representation X_r censored w.r.t. to S .*

The proof follows by observing that for sufficiently large D , X_r can be arbitrarily noisy, reducing (5) to an unconstrained optimization. For this X_r with $h^* = \operatorname{argmin}_h \mathbb{E}[\ell(h(X_r), S)]$,

$$\mathbb{E}[\ell(h^*(X_r); S)] = -\min_{g(\cdot)} \max_{h(\cdot)} -\mathbb{E}[\ell(h(g(\cdot)); S)] \quad (6)$$

$$\geq \mathbb{E}[\ell(h^*(g(\cdot)); S)], \quad (7)$$

thus satisfying Definition II.2.

The FUR framework in (5) places no restrictions on the adversary. Indeed, different loss functions and decision rules lead to different adversarial models (see Table D). This versatility

to a large class of (inferring) adversarial models is captured by the last entry in Table I by using the recently introduced tunable α -loss [23], [27], defined for $\alpha \in (0, 1) \cup (1, \infty)$ as :

$$\ell_\alpha(h(g(\cdot)), s) = \frac{\alpha}{\alpha - 1} \left(1 - P_h(s|g(\cdot))^{\frac{\alpha-1}{\alpha}} \right) \quad (8)$$

with continuous extensions at $\alpha = 1$ and $\alpha = \infty$. Note that the loss in (8) operates on a soft decision $P_h(\cdot|\cdot)$, the output of the adversary h . By tuning $\alpha \in [0, \infty]$, α -loss captures a variety of information-theoretic adversaries including:

(i) a hard-decision adversary for $\alpha = \infty$ captured by $\ell_\infty(h(g(\cdot)), s) = 1 - \Pr[h(g(\cdot)) \neq s]^2$, and

(ii) a soft-decision adversary for $\alpha = 1$ via the oft-used log-loss $\ell_1(h(g(\cdot)), s) = -\log P_h(s|g(\cdot))$,

thus subsuming the second and third entries in Table I. All other $\alpha > 1$ values allow interpolating between the NP-hard to implement MAP rule ($\alpha = \infty$) and log-loss ($\alpha = 1$) and allow some robustness to noisy data [23]. On the other hand, choosing $\alpha < 1$ leads to more convex losses than log-loss ($\alpha = 1/2$ yields a soft exponential loss used in boosting algorithms) that are more sensitive to outliers [23]. For any encoder $g(\cdot)$, the following proposition (see also the last row of Table I) summarizes the optimal $P_h^*(s|g(\cdot))$ under α -loss.

Proposition 2. *For a fixed g , under α -loss, the optimal adversary decision rule that minimizes the expected loss is a ‘ α -tilted’ conditional distribution $P_h^*(s|g(\cdot)) = \frac{P(s|g(\cdot))^\alpha}{\sum_{s \in \mathcal{S}} P(s|g(\cdot))^\alpha}$. For $\alpha = 1$ and $\alpha = \infty$, we obtain the optimal strategies for log-loss and 0-1 loss, respectively, as the true conditional distribution and the maximal a posteriori (MAP) estimator. Then, (5) reduces to $\min_{g(\cdot)} -H_\alpha^A(S|g(\cdot))$, where $H_\alpha^A(\cdot|\cdot)$ ³ is the Arimoto conditional entropy.*

Proposition 2 states that if the adversary uses ℓ_∞ or the 0-1 loss, (5) simplifies to $\min_{g(\cdot)} \max_{s \in \mathcal{S}} (P(s, g(\cdot)) - 1) = -1 + \min_{g(\cdot)} P_c(S|g(\cdot))$, where $P_c(S|g(\cdot))$ is the probability of correctly guessing S given $g(\cdot)$ [28]; if the adversary uses log-loss, (5) simplifies to $\min_{g(\cdot)} I(g(\cdot); S)$ for any prior on S , where $I(g(\cdot); S)$ is the mutual information (MI) between $g(\cdot)$ and S . More generally, using α -loss in (8), the optimal P_h^* in Proposition 2 simplifies the objective in (5) to $\min_{g(\cdot)} I_\alpha^A(g(\cdot); S)$, where $I_\alpha^A(g(\cdot); S)$ is the Arimoto MI⁴ of order α . These MIs can be effective proxies for guaranteeing DemP FURs, since they are minimized only when $S \perp g(\cdot)$, thus leading to the following theorem.

Theorem 2. *Under α -loss, for all α , (5) enforces fairness subject to a distortion constraint. As the distortion increases, the ensuing fairness guarantee approaches ideal DemP.*

We combine the proofs for Proposition 2 and Theorem 2 in Appendix B. Many notions of fairness require computing probabilities to ensure independence, and thus, are not easy to

²For $\alpha = \infty$, α -loss reduces to probability of error, for which the optimal rule that minimizes the expected loss is the *maximal a posteriori* (MAP) estimation, a hard decision. The same rule results when minimizing the 0-1 loss which is given by $\mathbb{I}(h(g(\cdot)) \neq s)$ where \mathbb{I} is the indicator function.

³ $H_\alpha^A(U|V) \triangleq 1/(1-\alpha) \log(\sum_{u,v} P_{U,V}^\alpha(u,v))$

⁴ $I_\alpha^A(g(\cdot); S) = H_\alpha(S) - H_\alpha^A(S|g(\cdot))$ where $H_\alpha(S) \triangleq H_\alpha^A(S)$ is the Rényi entropy of order α and is also the unconditioned α -Arimoto entropy.

optimize in a data-driven fashion. Theorem 2 justifies using α -loss (and thus, log-loss too) as a proxy for enforcing fairness.

A predominant approach in the literature in the context of fair representations is to explicitly include the intended classification task, i.e., design representations that guarantee DemP for the specific task [10]–[12]. In fact, the FUR formulation in (5) can be extended to include this case by adding an additional constraint to ensure high accuracy in learning Y . The resulting minimax game is given by

$$\begin{aligned} \min_{\tilde{g}(\cdot), f(\cdot)} \max_{h(\cdot)} & -\mathbb{E}[\ell(h(\tilde{g}(\cdot)), S)] + \lambda \mathbb{E}[\ell'(f(\tilde{g}(\cdot)), Y)], \quad (9a) \\ \text{s.t.} & \mathbb{E}[d(\tilde{g}(\cdot), X)] \leq D, \quad (9b) \end{aligned}$$

where $f(\cdot)$ is a classifier for a target Y , $\lambda > 0$, and $\tilde{g}(\cdot)$ ⁵ and $h(\cdot)$ are the encoder and the adversarial classifier, respectively, as in (5). Note that the loss functions $\ell(\cdot)$ and $\ell'(\cdot)$ can be different. The setup in (9) involves an additional constraint ensuring fair classification and is, thus, a more constrained optimization than the FUR framework; in fact, we recover the FUR setup with $\lambda = 0$. However, even while generating intermediate representations $g(\cdot)$, (9) is primarily intended to design *fair classifiers*, and therefore, requires knowing the intended tasks on Y . In contrast, our FUR framework allows generating DemP-guaranteeing fair X_r that in turn guarantee DemP fairness to all downstream tasks on any subset of Y .

One can also design fair classifiers directly without intermediate representations by setting $\tilde{g}(\cdot) \triangleq \hat{Y}$; such classifiers \tilde{g} can be designed with either DemP or EO guarantees. We first consider the more general problem of designing EO-fair predictors/classifiers $\tilde{g}(\cdot)$ for the target Y and show that our FUR framework subsumes this problem (and therefore, that of generating DemP predictors/classifiers). Let h be the adversary decision rule to infer S as $\hat{S} = h(\tilde{g}(\cdot), Y)$ using both Y and the soft predictor $\tilde{g}(\cdot) = P_{\hat{Y}|\cdot}$. Then, analogous to (5), the design of a fair predictor/classifier can be formulated as

$$\min_{\tilde{g}(\cdot)} \max_{h(\cdot)} -\mathbb{E}[\ell(h(\tilde{g}(\cdot), Y), S)], \text{ s.t. } \mathbb{E}[\ell(\tilde{g}(\cdot), Y)] \leq \epsilon. \quad (10)$$

Proposition 3. *Under α -loss, the formulation in (10) enforces EO fairness subject to a performance constraint ϵ . As ϵ increases, the ensuing fairness guarantee approaches the ideal EO guarantees achievable by \tilde{g} w.r.t. S and Y .*

The proof of Proposition 3 is in Appendix C. Note that the formulation in (10) also holds for generating a fair predictor/classifier satisfying DemP in Definition II.1. In contrast to EO where the adversary needs both $\tilde{g}(\cdot)$ and Y as inputs, for DemP, only $\tilde{g}(\cdot)$ is input to the adversary.

The adversarial models and the resulting game-theoretic solutions in Table I highlight the formal guarantees of the FUR framework. Recently, Sypherd *et al.* have demonstrated the robustness of training deep learning models with α -loss to both noise and class imbalances [23], thus promising to be applicable for learning FURs with GANs. The rest of the sequel focuses on data-driven GANs with $\alpha = 1$, i.e., log-loss, to highlight the value of FURs in guaranteeing fairness

⁵In general, $\tilde{g}(\cdot)$ can be a function of both X and S ; the dependence on S is implicit when S is not directly available.

	Loss function $\ell(h(g(\cdot)), s)$	Optimal adversarial strategy h^*	Adversary type
Squared loss	$(h(g(\cdot)) - S)^2$	$\mathbb{E}[S g(\cdot)]$	MMSE adversary
0-1 loss	$\begin{cases} 0 & \text{if } h(g(\cdot)) = S \\ 1 & \text{otherwise} \end{cases}$	$\operatorname{argmax}_{s \in \mathcal{S}} P(s g(\cdot))$	MAP adversary
Log-loss	$-\log P_h(s g(\cdot))$	$P(s g(\cdot))$	Belief refining adversary
α -loss	$\frac{\alpha}{\alpha-1} \left(1 - P_h(s g(\cdot))^{1-\frac{1}{\alpha}}\right)$	$\frac{P(s g(\cdot))^\alpha}{\sum_{s \in \mathcal{S}} P(s g(\cdot))^\alpha}$	Generalized belief refining adversary

Table I: The adversaries captured by the FUR framework by using a variety of loss functions.

for multiple downstream tasks relative to the state-of-the-art fair classifiers. Future work will include enhancing such results to include tuning over α .

B. Data-driven FUR

Thus far, we have focused on a setting where the curator has access to the statistics $P(X, S)$ thereby solving the constrained minimax optimization problem in (5) (game-theoretic version of the FUR formulation) to obtain a g that performs best against a chosen adversary. In practice, $P(X, S)$ is impossible to compute. To this end, we propose a data-driven version of the FUR formulation that allows the data holder to learn a generative decorrelator from an n -sample dataset $\mathcal{D} = \{(x_{(i)}, s_{(i)})\}_{i=1}^n$ via a generative model $g(X; \theta_p)$ that is parameterized by θ_p . This generative model takes X (or (X, S)) as input and outputs X_r . In the training phase, the data holder learns the optimal parameters θ_p by competing against a *computational adversary*: a classifier modeled by a neural network $h(g(X; \theta_p); \theta_a)$ that is parameterized by θ_a . In the evaluation phase, the performance of the learned decorrelation scheme can be tested under a strong adversary that is computationally unbounded and has access to dataset statistics. We follow this procedure in the next section.

While, in theory, the functions h and g can be arbitrary, in practice, they are best approximated by a well-chosen rich hypothesis class. Fig. 1 illustrates a FUR model in which h and g are both modeled as deep neural networks (DNNs). For a fixed h and g , binary S and $\ell = \ell_1$ (log-loss for $\alpha = 1$), the adversary's *empirical loss* using cross entropy is given by

$$L_n(\theta_p, \theta_a) = -\frac{1}{n} \sum_{i=1}^n s_{(i)} \log h(g(x_{(i)}; \theta_p); \theta_a) + (1 - s_{(i)}) \log(1 - h(g(x_{(i)}; \theta_p); \theta_a)). \quad (11)$$

The optimal model parameters (θ_p, θ_a) are then solutions of

$$\min_{\theta_p} \max_{\theta_a} -L_n(\theta_p, \theta_a), \text{ s.t. } \frac{1}{n} \sum_{i=1}^n d(g(x_{(i)}; \theta_p), x_{(i)}) \leq D. \quad (12)$$

The minimax optimization in (12) is a two-player non-cooperative game between the generative decorrelator and the adversary with strategies θ_p and θ_a , respectively. In practice, for chosen hypothesis classes for g and h (e.g., DNN architectures), we can learn the equilibrium of the game using an iterative algorithm as follows. (i) For a fixed θ_p , maximize the negative of the adversary's loss to compute the parameters of h . (ii) Then, minimize the decorrelator's loss (negative adversary loss) to compute θ_p for a fixed h .

It is crucial to note that the *hard* distortion constraint in (12) makes our minimax problem different from what

has been extensively studied in the literature. To incorporate the distortion constraint, we use the *penalty method* [21] to replace the constrained optimization problem by adding a penalty to the objective function. This is done via a penalty parameter ρ_t that scales a measure of violation of the constraint at the t^{th} iteration. The constrained optimization problem of g is then approximated by a *series of unconstrained optimization problems* with an objective $L_n(\theta_p, \theta_a) + \rho_t (\max\{0, \frac{1}{n} \sum_{i=1}^n d(g(x_{(i)}; \theta_p), x_{(i)}) - D\})^2$, where the penalty coefficient ρ_t increases with the number of iterations t . The algorithm and the penalty method are detailed in Appendix D. Finally, we note that one can easily generalize (11) to the multi-class setting (non-binary S) using the softmax function; one can also generalize (11) using α -loss.

In the following sections, we detail our results for synthetic multi-dimensional Gaussian mixture data and two publicly available datasets: UCI Adult and UTKFace. All code is available via GitHub at [29]. Results for GENKI and Human Activity Recognition (HAR) are in the supplement.

IV. FUR FOR GAUSSIAN MIXTURE MODELS

In this section, we focus on a setting where $S \in \{0, 1\}$ and X is an m -dimensional Gaussian mixture random vector whose mean is dependent on S . Let $P(S = 1) = q$. Let $X|S = 0 \sim \mathcal{N}(-\mu, \Sigma)$ and $X|S = 1 \sim \mathcal{N}(\mu, \Sigma)$, where $\mu = (\mu_1, \dots, \mu_m)$. Without loss of generality, we assume that $X|S = 0$ and $X|S = 1$ have the same covariance Σ .

A. Game-Theoretical Approach

We consider a MAP adversary that has access to $P(X, S)$ and g . The goal is to censor X in a way that minimizes the adversary's probability of correctly inferring S from X_r . In order to have a tractable model for the encoder, we mainly focus on affine representations $X_r = g(X) = X + Z + \beta$, where for tractability reasons, we choose Z as a zero-mean multi-dimensional Gaussian random vector independent of X . This linear representation enables controlling both the mean and covariance of X_r . To quantify utility of the privatized data, we use the ℓ_2 distance between X and X_r as a distortion measure to obtain a constraint $\mathbb{E}_{X, X_r} \|X - X_r\|^2 \leq D$.

Without loss of generality, we assume that $\beta = (\beta_1, \dots, \beta_m)$ is a constant parameter vector and $Z \sim \mathcal{N}(0, \Sigma_p)$. For the standard Gaussian $Q(\cdot)$ function, we can derive the adversary's detection probability $P_d^{(G)}$ as

$$P_d^{(G)} = qQ\left(-\frac{\gamma}{2} + \frac{1}{\gamma} \ln\left(\frac{1-q}{q}\right)\right) + (1-q)Q\left(-\frac{\gamma}{2} - \frac{1}{\gamma} \ln\left(\frac{1-q}{q}\right)\right), \quad (13)$$

where $\gamma = \sqrt{(2\mu)^T(\Sigma + \Sigma_p)^{-1}2\mu}$. From the constraint, we have $\mathbb{E}_{X, X_r} \|X - X_r\|^2 = \|\beta\|^2 + \text{tr}(\Sigma_p) \leq D$. The following theorem summarizes the optimal noising strategy when $X|S$ and Z are multi-dimensional Gaussians.

Theorem 3. Consider the representation given by $g(X) = X + Z + \beta$, where $X|S$ and Z are Gaussian random vectors with diagonal covariance matrices Σ and Σ_p , respectively, and $X|S \perp Z$. Let $\{\sigma_1^2, \dots, \sigma_m^2\}$ and $\{\sigma_{p_1}^2, \dots, \sigma_{p_m}^2\}$ be the diagonal entries of Σ and Σ_p , respectively. The parameters of the minimax optimal censoring mechanism g^* are

$$\beta_i^* = 0, \quad \sigma_{p_i}^{*2} = \left(\frac{|\mu_i|}{\sqrt{\lambda_0^*}} - \sigma_i^2 \right)^+, \quad \forall i = \{1, 2, \dots, m\},$$

where λ_0^* , the dual variable enforcing the distortion constraint in (5), is chosen such that $\sum_{i=1}^m \sigma_{p_i}^{*2} = D$. For this optimal mechanism, the accuracy of the MAP adversary is given by (13) with $\gamma = 2\sqrt{\sum_{i=1}^m \mu_i^2 / (\sigma_i^2 + \sigma_{p_i}^{*2})}$.

The proof of Theorem 3 is in Appendix E. We observe that when $\sigma_i^2 > |\mu_i|/\sqrt{\lambda_0^*}$, no noise is added to the data on this dimension due to the high variance. In contrast, when $\sigma_i^2 < |\mu_i|/\sqrt{\lambda_0^*}$, the variance of the noise added to this dimension is proportional to $|\mu_i|$; this is intuitive since a large $|\mu_i|$ indicates the two conditionally Gaussian distributions are further away on this dimension, and thus, require more noise to reduce the MAP adversary's inference accuracy.

B. Data-driven Approach

To learn the data-driven representation $X_r = g(X) = X + Z + \beta$ using our FUR framework, we assume that g only has access to the dataset \mathcal{D} with n data samples (not $P(X, S)$). Computing the optimal g^* is then a learning problem. In the training phase, we learn the parameters θ_p of g by competing against a computational adversary $h(g(\theta_p); \theta_a)$ modeled by a multi-layer neural network. When convergence is reached, we evaluate the performance of the learned mechanism by comparing with the one obtained from the game-theoretic approach. To quantify the performance of the learned X_r , we compute the accuracy of inferring S under a strong MAP adversary that has access to both the joint distribution of (X, S) and the censoring mechanism.

Since the sensitive variable S is binary, we measure the training loss of the adversary network using the empirical log-loss function in (11). As shown in Fig. 2, we model the encoder using a two-layer neural network with parameters $\theta_p = \{\beta_1, \dots, \beta_m, \sigma_{p_1}, \dots, \sigma_{p_m}\}$, where β_k and σ_{p_k} represent the mean and standard deviation for each dimension $k \in \{1, \dots, m\}$, respectively. The random noise Z is drawn from a m -dimensional independent zero-mean standard Gaussian distribution with covariance $\Sigma_p = \text{diag} \sigma_{p_1}^2, \dots, \sigma_{p_m}^2$. Thus, $\hat{X}_k = X_k + \beta_k + \sigma_{p_k} Z_k$. The adversary is modeled by a three-layer neural network classifier with leaky ReLU activations. Finally, as detailed in Algorithm 1, we use the penalty method to ensure the distortion constraint.

C. Illustration of Results

We generate two synthetic datasets to illustrate our results; each dataset has 20K training samples and 2K test samples.

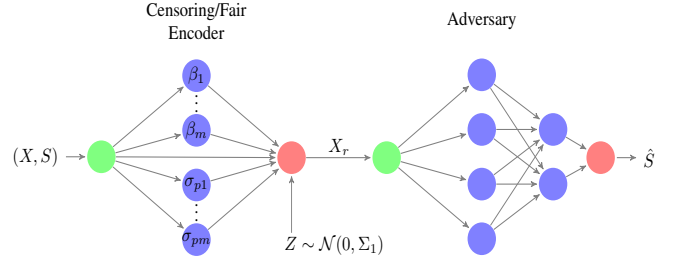


Figure 2: Neural network structure for a m -dimensional Gaussian $X|S$ to learn $\{\beta\}_{j=0}^m$ and $\{\sigma\}_{j=0}^{p_m}$ for $X_r = X + Z + \beta$.

Each dataset is generated by sampling from an independent multi-dimensional Gaussian mixture model. The two datasets correspond to two distinct values for the prior $P(S = 1)$ as 0.75 and 0.5. Both the encoder and the adversary in the FUR framework are trained on Tensorflow [30] using the Adam optimizer [31] with a learning rate of 0.005 and a minibatch size of 1000. The distortion constraint is enforced by the penalty method as detailed in Appendix D (see (23)).

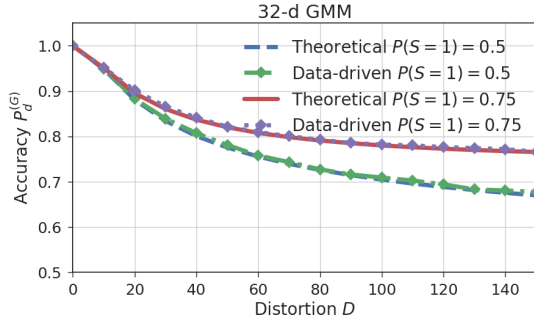
Fig. 3 illustrates the performance of the learned FUR scheme against a strong theoretical MAP adversary for a 32-dimensional Gaussian mixture model with $P(S = 1) = 0.75$ and 0.5. We observe that the inference accuracy of the MAP adversary decreases as the distortion increases and asymptotically approaches (as expected) the prior $P(S = 1)$. The decorrelation scheme obtained via the data-driven approach performs very well when pitted against the MAP adversary (maximum accuracy difference around 0.7% compared to the theoretical optimal). Furthermore, the estimated MI decreases as the distortion increases. In other words, for the data generated by Gaussian mixture model with binary sensitive variable, the data-driven FUR formulation can learn decorrelation schemes that perform as well as those computed under the game-theoretical FUR formulation where the generative decorrelator has access to the data statistics.

V. FUR FOR PUBLICLY AVAILABLE DATASETS

We apply our FUR framework to real-world datasets including GENKI, HAR, UCI Adult, and UTKFace. The GENKI and HAR datasets and results are detailed in the supplement:

- (i) The UCI Adult dataset [32] consists of 10 categorical and 4 continuous features and is used to predict a binary salary label (1: salary > 50k or 0: salary ≤ 50k). We choose gender or the tuple (gender, relationship) as the sensitive S , the remaining features except salary as non-sensitive X (Table SIV in the supplement lists all features), and salary as the target Y .
- (ii) The UTKFace dataset [33] consists of more than 20k 200 × 200 color images of faces labeled by age, ethnicity, and gender. Individuals in the dataset have ages from 0 to 116 years and are divided into 5 ethnicities: White, Black, Asian, Indian, and others including Hispanic, Latino and Middle Eastern. We take gender as S , the image as X , and age and ethnicity as two target labels Y . Further, we also restrict the data to contain images for ages between 10 and 65.

We use the accuracy of predicting S as the measure of censoring. We evaluate the fairness guarantees of X_r by



(a) Sensitive variable classification accuracy

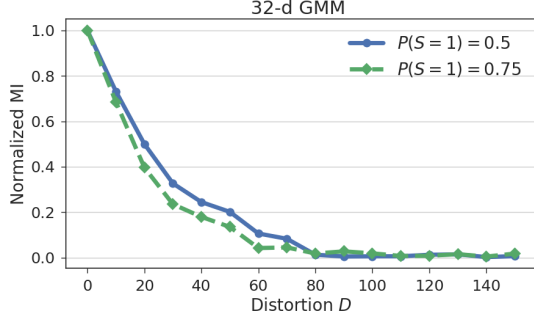
(b) Estimated mutual information between S and \hat{X}

Figure 3: Performance of the FUR framework for Gaussian mixture models.

computing the DemP obtained on tasks using Y . To this end, we compute the following maximal difference as a proxy for DemP in Definition II.1 (includes non-binary Y and S):

$$\Delta_{\text{DemP}}(y) = \max_{s, s' \in \mathcal{S}} |P(\hat{Y}=y|S=s) - P(\hat{Y}=y|S=s')| \quad (14)$$

with smaller values of Δ_{DemP} suggesting better DemP fairness guarantees. We illustrate both censoring and fairness results for the abovementioned datasets in the following subsections. Experimental and model details are in the supplement.

A. Illustration of Results for UCI Adult Dataset

For the UCI Adult dataset with both categorical and continuous features as shown in Table SIV in the supplement, we consider two cases:

- (i) Case I: binary S by choosing ‘gender’ as sensitive feature
- (ii) Case II: non-binary S by considering both ‘gender’ and ‘relationship’ as sensitive. For UCI, ‘relationship’ has 6 distinct values, and therefore, S has 12 possibilities.

For both cases, ‘salary’ is the binary target $Y \in \{0, 1\}$, with $Y = 1$ denoting salary $> 50K$. For binary Y , $\Delta_{\text{DemP}}(y)$ in (14) simplifies to a single value that we denote as Δ_{DemP} .

Case I: Binary Sensitive Feature.

Fig. 4 illustrates the censoring and fairness performance of the generated X_r for the UCI dataset. For censoring, the performance is evaluated via the tradeoff between the classification accuracies of salary (utility of X_r) and gender (censoring of S). We evaluate fairness via the tradeoff between salary accuracy and Δ_{DemP} . We consider two possible inputs to the encoder $g(\cdot)$ in (5), i.e., only X or both (X, S) .

As illustrated in Fig. 4a, the baseline⁶ salary and gender accuracies for the UCI dataset are about 84.5% and 85%, respectively. Further, for the FUR X_r and downstream \hat{Y} : (i) the smallest gender accuracy achievable is about 66%, 20% below its baseline, while the lowest salary accuracy is about 82%, 2.5% below its baseline. Since the likelihood of a male in the original test data is 66%, with increasing distortion, the FUR gender accuracy is as good as a random guess, i.e., the generated X_r hides gender effectively while maintaining high salary accuracy.

(ii) For the same gender accuracy, using both (X, S) seems useful only in the high utility setting (salary accuracy $\geq 83\%$).

From Fig. 4b, we make the following two observations: (i) salary classification accuracy and Δ_{DemP} have an approximately affine relationship, and when $\Delta_{\text{DemP}} \approx 0$, the salary accuracy is $\geq 79\%$, i.e., the FUR framework is effective in approaching perfect DemP with a small reduction in utility; (ii) the representations X_r generated from either X or (S, X) lead to similar fairness guarantees. For $\Delta_{\text{DemP}} = 0.06$, while state-of-the-art approaches in [12] and [11] achieve 2% and 2.5% higher salary accuracy than ours, our approach is distinct in achieving $\Delta_{\text{DemP}} \approx 0$ with salary accuracy $\geq 79\%$.

We can also evaluate the fairness performance of the generated X_r by using the EO measure in Definition II.1. Thus, for $Y \in \{0, 1\}$ where $Y = 1$ when salary $> 50K$, $S \in \{0, 1\}$ (female:1 and male:0), and $\hat{Y} \in \{0, 1\}$, we write $\Delta_{\text{EO}}(y)$, $\forall y \in \{0, 1\}$ as:

$$\Delta_{\text{EO}}(y) \triangleq \left| P(\hat{Y}=y|S=0, Y=y) - P(\hat{Y}=y|S=1, Y=y) \right| \quad (15)$$

From Fig. 5, we observe that while the salary accuracy is above 82.4%, the values of $\Delta_{\text{EO}}(1)$ and $\Delta_{\text{EO}}(0)$ decrease to 0.0007 and 0.0254, respectively. To understand the significance of these results, we compare against the state-of-the-art in [11], wherein fair salary classifiers for both DemP and EO measures, referred to as LAFTR-DP⁷ and LAFTR-EO, respectively, are learned for the UCI dataset. For the LAFTR-DP, the authors also compute the resulting EO of the DemP classifier. Specifically, when $\Delta_{\text{EO}}(1) + \Delta_{\text{EO}}(0) = 0.04$ ⁸, our salary accuracy is 1.3% smaller than that achieved by LAFTR-DP (cf. Fig. 2(b) in [11]), but our minimal achieved value of $\Delta_{\text{EO}}(1) + \Delta_{\text{EO}}(0)$ is only 72% of that achieved by LAFTR-DP and is the same as the value achieved by LAFTR-EO, which uses EO as the fairness metric to train a salary classifier. In addition, we observe that the decrease of $\Delta_{\text{EO}}(1) + \Delta_{\text{EO}}(0)$ is even larger than Δ_{DemP} . That is, even though the representation is generated to satisfy DemP, it can also provide competitive downstream EO fairness guarantees. This, in turn, justifies the rationality of generating fair representations under DemP.

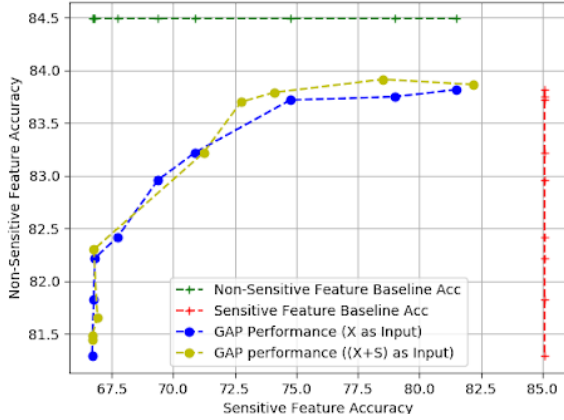
Case II: Non-binary Sensitive Feature.

Figs. 6 and 7 illustrate the censoring and fairness performances of the generated X_r in hiding ‘gender’ and ‘relationship’, respectively, while preserving ‘salary’ information. Fig. 6 illustrates the tradeoff between salary and sensitive feature

⁶The baseline performances are the salary and gender accuracies as well as Δ_{DemP} obtained from the original uncensored test dataset.

⁷Learned Adversarially Fair and Transferable Representations (LAFTR)

⁸[11] introduced an EO measure as $\Delta_{\text{EO}} \triangleq \Delta_{\text{EO}}(1) + \Delta_{\text{EO}}(0)$



(a) Salary vs. gender classification accuracy

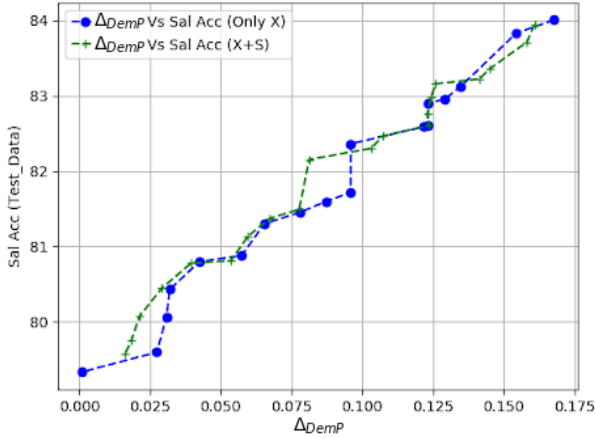
(b) Salary classification accuracy vs. Δ_{DemP}

Figure 4: Results for UCI Adult: Case I. In Fig. 4a, the green and red lines denote the baseline performances for the target Y (salary) and sensitive S (gender), respectively; in Fig. 4b, the value of Δ_{DemP} for the original test data is 0.2.

S accuracies when S is either gender, or relationship, or both. From Fig. 6, we observe that while the salary accuracy is above 79%, the classification accuracies of gender and/or relationship are about 66% (Fig. 6a), 45% (Fig. 6b) and 41% (Fig. 6c), respectively. Note that the probabilities of male, husband, and the combination (male, husband) are 66%, 40% and 40%, respectively, in the original test data. Therefore, while the salary accuracy is preserved at 79%, the inferences of gender, relationship, and combination (gender, relationship) approach random guessing with these priors. Thus, our FUR framework can effectively hide one or more sensitive features. However, suppressing multiple correlated sensitive features comes at a cost of a reduction in salary accuracy. Thus, comparing Figs. 4a and 6a, we see a maximal reduction of 3% in salary accuracy for a given gender accuracy⁹.

For Case II, Figs. 7a and 7b illustrate the tradeoffs between the salary accuracy and Δ_{DemP} for S chosen as gender or relationship or both. We observe that while salary accuracy is above 94% of the baseline performance, the value of Δ_{DemP}

⁹In Figs., 4a and 6a, the baseline performances are different because for Case II, the feature variable X does not contain ‘relationship’.

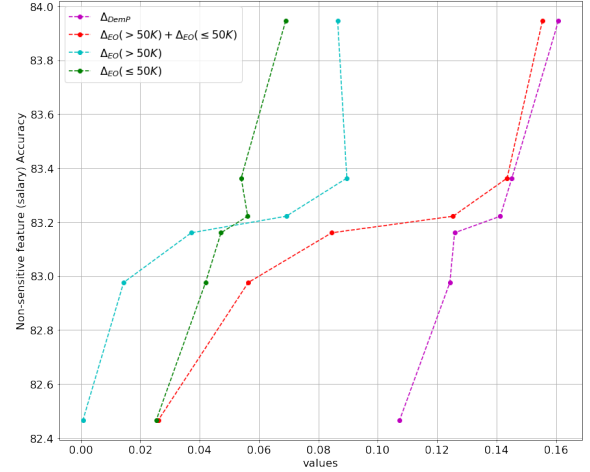


Figure 5: Evaluation of equalized odds fairness metric under Case I for the UCI Adult dataset. The EO measures $\Delta_{\text{EO}}(1)$ and $\Delta_{\text{EO}}(0)$ are defined in (15). The red curve plotting $\Delta_{\text{EO}} = \Delta_{\text{EO}}(1) + \Delta_{\text{EO}}(0)$ matches Δ_{EO} in Figure 2(b) of [11].

is dropped to 25% for gender and to about 34% for both relationship and their combination. In short, X_r works well in decorrelating gender and relationship both separately and jointly without affecting downstream classifier performance. From Fig. 7b, we observe that the value of Δ_{DemP} for the combination is almost the same as that for relationship. In addition, comparing the results in Figs. 4b and 7b, for any given salary accuracy, Δ_{DemP} for gender in Case II is about 25% higher than that in Case I; this can be viewed as the cost of enforcing fairness for the non-binary relationship feature.

B. Illustration of Results for UTKFace Dataset

In the UTKFace dataset, the face images are the non-sensitive X . We choose ‘gender’ as the sensitive S ; focusing on multiple downstream tasks, we consider both ethnicity classification and age regression, for which we choose ‘ethnicity’ or ‘age’ as the target variable Y , respectively. For the two downstream applications, the corresponding supports of Y are $\mathcal{Y} = \{\text{White, Black, Asian, Indian}\}$ and $\mathcal{Y} = \{i \in \mathbb{Z} : 10 \leq i \leq 65\} = [10, 65]$, respectively. We use the maximum of the DemP measure (defined in (14)) over the support Y , i.e., $\Delta_{\text{DemP}} = \max_{y \in \mathcal{Y}} \Delta_{\text{DemP}}(y)$, as the achieved fairness level.

Fig. 8 illustrates the output X_r for 16 typical¹⁰ faces in the UTKFace dataset for increasing per-pixel distortion. From Fig. 8, we observe that: (i) for a small per-pixel distortion (e.g., 0.003), gender-distinguishing features such as lip color are smoothed out; and (ii) at higher per-pixel distortion (e.g., 0.006), the FUR framework can generate a face with an opposite gender (see the highlighted examples in Fig. 8) thereby completely obfuscating this sensitive feature; (iii) when the average per-pixel distortion is too large (e.g., 0.01), the representations generated are often too blurred.

Figs. 9a and 10 show the tradeoffs between gender classification accuracy and appropriate measures for ethnicity

¹⁰The 16 typical faces covers the 8 possible combination of 2 gender (male and female) and 4 ethnicities (White, Black, Asian and Indian) and includes young, adult and old faces.

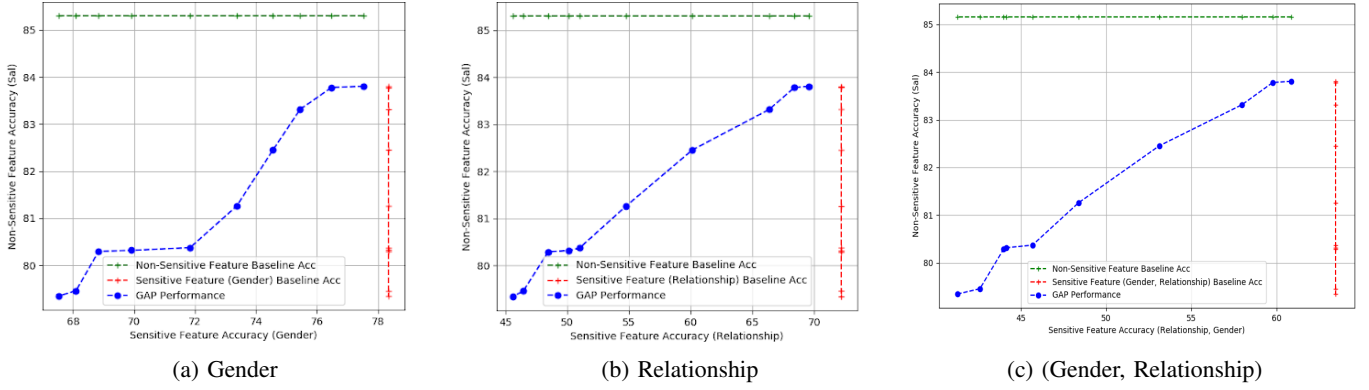


Figure 6: Tradeoff between classification accuracy of non-sensitive feature (salary) and sensitive features (gender and/or relationship) under Case II for the UCI Adult dataset. Note that we use the classification accuracy obtained from the original testing dataset as the baseline performance, which is denoted by the green and red lines for the target variable (salary) and the sensitive variable (gender or/and relationship), respectively.

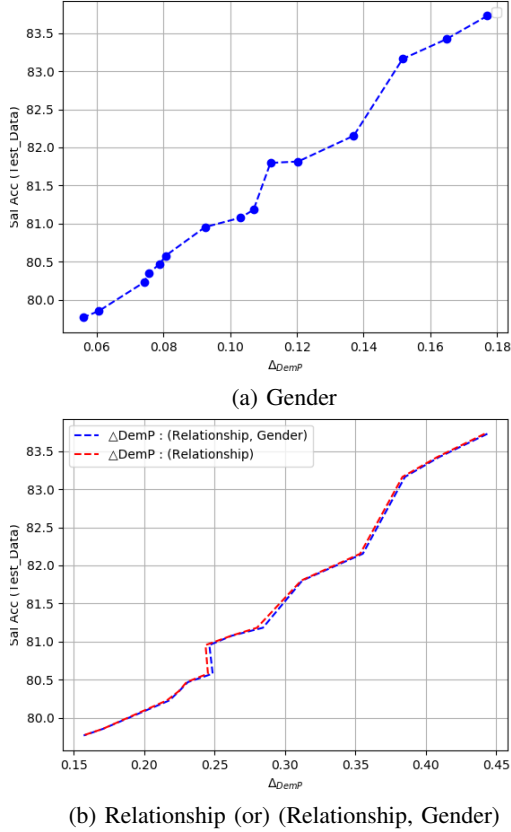


Figure 7: Case II for UCI Adult: Tradeoffs between salary accuracy and the Δ_{DemP} of gender and/or relationship. For the original test data, Δ_{DemP} for gender, relationship and the pair (gender, relationship) is 0.2, 0.438 and 0.443, respectively.

classification and age regression, respectively. In Fig. 9a, while gender classification accuracy is about 62% and decreases about 35% from the baseline performance, the classification accuracy of ethnicity is above 74% and only decreases 14% from its baseline performance. Note that in the original testing data, the highest marginal probabilities for gender and ethnicity are 54.6% (likelihood of male) and 43.2% (likelihood

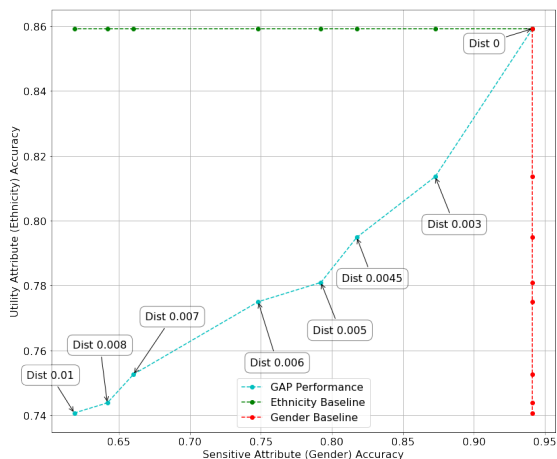


Figure 8: The encoded face images for different values of pixel distortions for the UTKFace dataset. Set of vertical faces highlighted in boxes make explicitly how the sensitive feature (gender) is changed with increasing distortion.

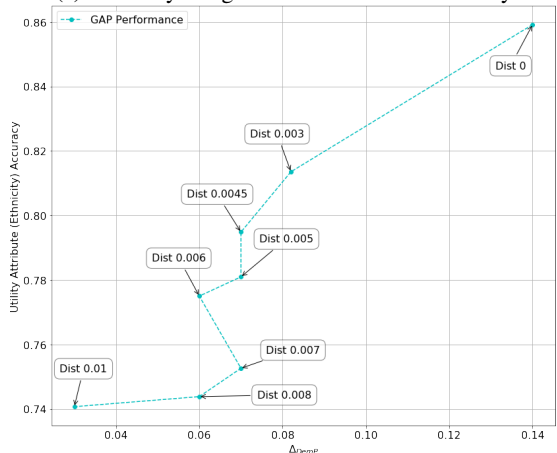
of White), respectively. Therefore, gender accuracy is better than a random guess by only 7.4% while ethnicity accuracy is better than a random guess by 30.8%, i.e., the generated X_r hides gender information well while maintaining ethnicity. For age regression, we use the mean absolute error (MAE), i.e., the average absolute difference between the predicted age and the true age, as the utility measure. In Fig. 10a, we observe that while the classification accuracy for gender is about 62%, which is a 35% decrease from the baseline performance of 94%, the increase in the MAE is 1.5 which is about a 20% increase from the baseline performance of 7.2 years. Fig. 10b shows the cumulative distribution function (CDF) of the difference between the true and predicted age for various distortions, from which we can see that the drop of the cumulative probability is at most 1%. Thus, the generated FUR guarantees reliable performance for both age and ethnicity prediction; thus, constraining the distortion of the generated X_r can be effective in guaranteeing utility for multiple tasks.

In Figs. 9b and 11, we illustrate the tradeoff between the

utility measure and Δ_{DemP} of the generated X_r in ethnicity classification and age regression, respectively. In Fig. 9b, we observe that while achieving about 86% of the baseline classification accuracy, the Δ_{DemP} is reduced to 0.03, which is 20% of the $\Delta_{\text{DemP}} = 0.14$ in the original testing data. Table II shows the decrease of Δ_{DemP} for each of the four ethnicities as the distortion increases. In Fig. 11a, while preserving 86% of the utility baseline performance, the Δ_{DemP} , i.e., the maximal value of demographic parity measure over the 56 age values, decreases to 0.015, which is less than 33% of the $\Delta_{\text{DemP}} = 0.046$ in the original testing data. Fig. 11b shows the demographic measure $\Delta_{\text{DemP}}(y)$, $y \in [10, 65]$, for various distortions; we observe that when the pixel distortion is 0.01, even while $\Delta_{\text{DemP}} = 0.015$, $\Delta_{\text{DemP}}(y) = 0$ for 17 distinct ages. That is, the predictions of these 17 ages are completely independent of gender and DemP is achieved for those predictions.



(a) Ethnicity vs. gender classification accuracy

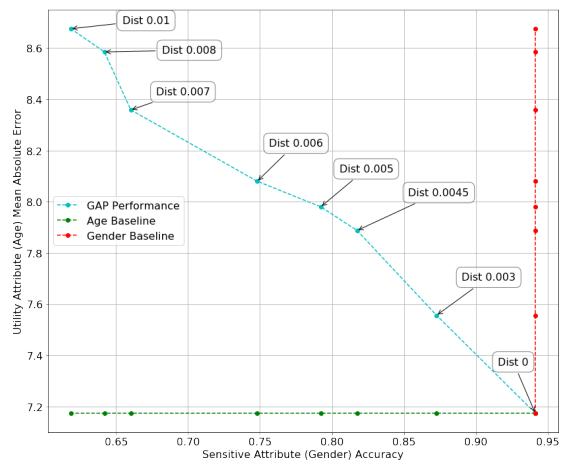


(b) Ethnicity classification accuracy vs. Δ_{DemP}

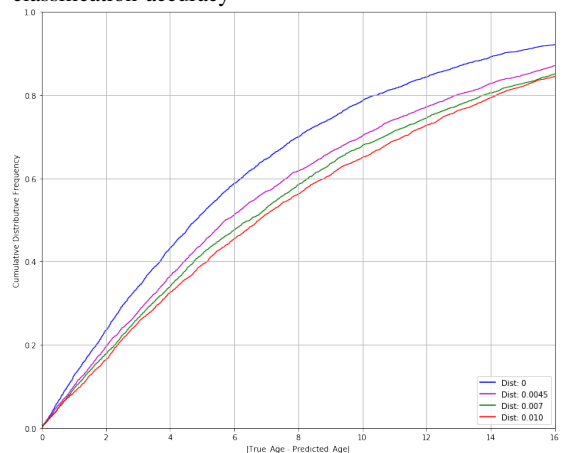
Figure 9: Ethnicity classification accuracy vs. gender classification and Δ_{DemP} for the UTKFace dataset. Note that in Fig. 9b, the x-axis is the maximal value of demographic parity measure in (14) over the four ethnicities and ‘dist’ indicates the per pixel distortion on images.

VI. CONCLUSION

We have introduced an adversarial learning framework with verifiable guarantees for learning generative models that can



(a) Mean absolute error of age prediction vs. gender classification accuracy



(b) The CDF of the difference between the true and predicted age

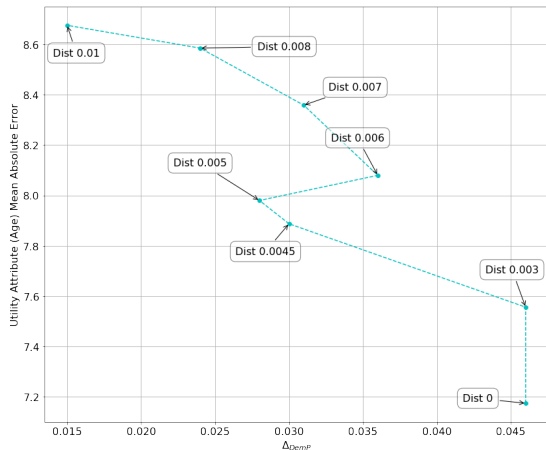
Figure 10: Utility of age regression on the UTKFace dataset. Note that ‘dist’ indicates the per pixel distortion on images.

create censored and fair universal representations for datasets with known sensitive features. The novelty of our approach is in producing representations that are fair with respect to the sensitive features for any *a priori* unknown downstream learning task. We have shown that our FUR framework allows the data holder to learn the fair encoding scheme (a randomized mapping that decorrelates the sensitive and non-sensitive features) directly from the dataset without requiring access to dataset statistics. One of our key results is that for appropriately chosen loss functions, the minimax game generating FURs can provide guarantees against strong information-theoretic adversaries, such as MAP (0-1 loss) and MI (log-loss) adversaries. We have also shown that our framework also allows approaching (ideal) demographic parity fairness using a tunable class of α -loss functions (which includes both log-loss and 0-1 loss) that capture a range of adversarial actions. For the setting with a known classification task, we have also shown that our FUR framework can be modified to approximate either DemP or EO fairness measures.

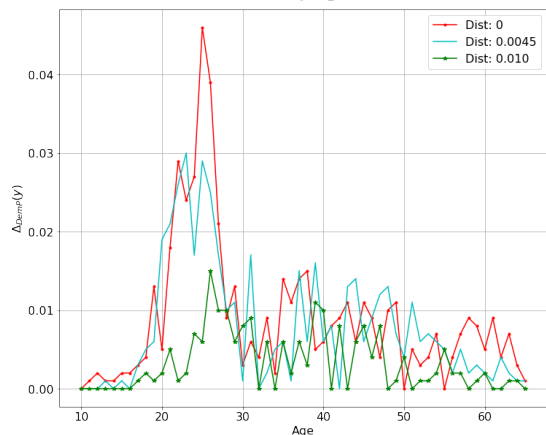
Finally, we have also validated the performance of the FUR framework on both synthetic and publicly available

Distortion	0	0.003	0.0045	0.005	0.006	0.007	0.008	0.01
$\Delta_{\text{DemP}}(\text{White})$	0.061	0.055	0.04	0.03	0.03	0.02	0.02	0.01
$\Delta_{\text{DemP}}(\text{Black})$	0.109	0.021	0.02	0.05	0.03	0.05	0.03	0.03
$\Delta_{\text{DemP}}(\text{Asian})$	0.14	0.082	0.07	0.07	0.06	0.07	0.06	0.03
$\Delta_{\text{DemP}}(\text{Indian})$	0.031	0.006	0.01	0	0.01	0	0.01	0.01

Table II: Demographic parity fairness (indicated by $\Delta_{\text{DemP}}(\cdot)$) of ethnicity classification on the UTKFace dataset.



(a) Mean absolute error of age prediction vs. Δ_{DemP}



(b) The demographic parity measure for various distortions

Figure 11: Achieved demographic parity for the age regression task on the UTKFace dataset. Note that in Fig. 11a, the x-axis is the maximal value of demographic parity measure in (14) over the chosen age range (10-65) and ‘dist’ indicates the per pixel distortion on images.

real datasets, including Gaussian mixture models, images, and datasets involving a mix of categorical and continuous features. Our results have allowed us to visually highlight three key results: (a) the tradeoff between representation fidelity and censoring guarantees (via accuracy in adversarially learning sensitive features); (b) the tradeoff between the adversarial accuracy in learning the sensitive features and the accuracy of multiple downstream tasks learned from the censored representation for a variety of datasets; and (c) the tradeoff between accuracy for a downstream learning task and the DemP or EO guarantees achieved by a predictor that is learned using

a DemP fair representation. Result (c) further suggests that, for some datasets, DemP FURs do not adversely affect the downstream EO guarantees despite lack of access to the task labels Y , where the latter has been highlighted as a limitation of DemP fair predictors [8]. However, more work is needed to understand the conditions under which DemP FURs suffice to achieve meaningful EO guarantees.

Going beyond this work, there are several fundamental questions that we seek to address. An immediate one is to explore the robustness of using α -loss (for $\alpha \neq 1$) in ensuring censoring and fairness for highly imbalanced datasets. More broadly, it will be interesting to investigate the robustness and convergence guarantees of the generative encoder learned in a data-driven fashion.

VII. ACKNOWLEDGEMENT

We would also like to thank Prof. Ram Rajagopal and Xiao Chen at Stanford for their help with estimating mutual information for the GENKI and HAR datasets, and would like to thank Mit Patel and Harshit Laddha at ASU for their help with the experiments on the UTKFace datasets.

APPENDIX

A. Proof for Theorem 1

A demographically fair encoder $g(X, S)$ ensures that $X_r \perp S$, i.e., the mutual information $I(S; X_r) = 0$. Further, the downstream learning algorithm acts only on X_r to predict \hat{Y} ; thus, $(S, X) - X_r - \hat{Y}$ form a Markov chain. From the data processing inequality and non-negativity of mutual information, we have $0 \leq I(S; \hat{Y}) \leq I(S; X_r) = 0$, i.e., S is independent of \hat{Y} ; thus, from Definition II.1, \hat{Y} satisfies DemP w.r.t. S . Finally, from the chain rule and non-negativity of mutual information, we have $I(X_r; S_t) = 0$ for any $S_t \subset S$, i.e., \hat{Y} satisfies DemP w.r.t. any subset of sensitive features S_t .

B. Proofs of Proposition 2, Results in Table I, and Theorem 2

In the FUR framework, different loss functions and decision rules lead to different adversarial models. We now prove the optimal adversarial rule for different loss functions in Table I.

Hard Decision Rules. When the adversary adopts a hard decision rule, $h(g(X))$ is an estimate of S . Under this setting, we can choose $\ell(h(g(X)), S)$ in a variety of ways. For instance, if S is continuous, the adversary can attempt to minimize the difference between the estimated and true sensitive variables using a squared loss (ℓ_2 loss) as

$$\ell(h(g(X)), S) = (h(g(X)) - S)^2. \quad (16)$$

One can verify that the optimal $h^* = \mathbb{E}[S|g(X)]$, the conditional mean of S given $g(X)$. Then, (5) simplifies to

$$\min_{g(\cdot)} -\text{mmse}(S|g(X)) = -\max_{g(\cdot)} \text{mmse}(S|g(X)),$$

subject to the distortion constraint and mmse is the minimum mean square error (MMSE). Thus, for the ℓ_2 loss, the FUR framework provides censoring guarantees against an MMSE adversary. On the other hand, when S is discrete (e.g., age, gender, etc.), the adversary can maximize its classification accuracy by considering the 0-1 loss [34] given by

$$\ell(h(g(X)), S) = \begin{cases} 0 & \text{if } h(g(X)) = S \\ 1 & \text{otherwise.} \end{cases} \quad (17)$$

One can verify that the adversary's optimal strategy is the maximum *a posteriori* probability (MAP) rule: $h^* = \operatorname{argmax}_{s \in \mathcal{S}} P(s|g(X))$, with ties broken uniformly at random. For this MAP rule, the objective in (5) reduces to

$$\min_{g(\cdot)} -(1 - \max_{s \in \mathcal{S}} P(s, g(X))) = \min_{g(\cdot)} \max_{s \in \mathcal{S}} P(s, g(X)) - 1,$$

i.e., under 0-1 loss, the FUR formulation provides censoring guarantees against a MAP adversary.

Soft Decision Rules. Instead of a *hard decision*, we can also consider a broader class of *soft decision* rules where $h(g(X))$ is a distribution over \mathcal{S} ; i.e., $h(g(X)) = P_h(s|g(X))$ for $s \in \mathcal{S}$. We first consider log-loss given by

$$\ell(h(g(X)), s) = \log \frac{1}{P_h(s|g(X))}. \quad (18)$$

In this case, the objective of the adversary simplifies to

$$\max_{h(\cdot)} -\mathbb{E} \left[\log \frac{1}{P_h(s|g(X))} \right] = -H(S|g(X)),$$

where $H(X|Y)$ is the conditional entropy of X given Y and, given the true posterior $P(s|g(X))$, $P_h^*(s|g(X)) = P(s|g(X))$. Then, the objective in (5) reduces to

$$\min_{g(\cdot)} -H(S|g(X)) = \min_{g(\cdot)} I(g(X); S) - H(S), \quad (19)$$

i.e., under log-loss, the FUR formulation is equivalent to using mutual information as the censoring (or privacy) metric.

Tunable α -loss family. For $\ell(h(g(x)), s)$ chosen as α -loss in (8), since α -loss is convex in $P_h(s|g(X))$ [27], we have

$$\max_{h(\cdot)} -\mathbb{E}[\ell(h(g(X)), S)] = \frac{\alpha}{1-\alpha} \left(1 - e^{(\frac{1-\alpha}{\alpha} H_\alpha^A(S|g(X)))} \right)$$

where $H_\alpha^A(\cdot|\cdot)$ is the Arimoto conditional entropy of order α ; the optimal h^* is a ' α -tilted' conditional distribution

$$P_h^*(s|g(X)) = P(s|g(X))^\alpha / \sum_{s' \in \mathcal{S}} P(s'|g(X))^\alpha. \quad (20)$$

For this P_h^* , the objective in (5) reduces to

$$\min_{g(\cdot)} I_\alpha^A(S; g(X)) - H_\alpha(S), \quad (21)$$

where $H_\alpha(S)$ is the Rényi entropy of order α . For $\alpha = 1$, (21) simplifies to (19) since the Arimoto conditional entropy (resp. MI) simplifies to the Shannon conditional entropy (resp. MI) [35]. From the non-negativity of Arimoto MI $I_\alpha^A(S; g(X))$, we also have $H_\alpha^A(S|g(X)) \leq H_\alpha(S)$ [35] with equality if and only if $g(X)$ is independent of S . Thus, the minimization in (21) serves as a proxy for generating DemP fair representations with perfect DemP achieved when $I_\alpha^A = 0$.

Near perfect DemP is achievable for very large distortions

as this allows X_r to be increasingly decoupled from S and X . Indeed, as the bound D in (5) increases, from Proposition 1, the FUR formulation in (5) will *approach* ideal DemP by achieving $I_\alpha^A(S|g(X)) \approx 0$, thus proving Theorem 2.

C. Proof for Proposition 3

The optimization in (10) differs from that in (5) in including the target Y in learning both g and h^* . In fact, for a fixed g , one can verify that the optimal adversarial strategy in (10) is the same as (20) with an additional conditioning on Y . Thus, for $\ell = \ell_\alpha$ in (8), the optimization in (10) reduces to

$$\min_{g(\cdot)} I_\alpha^A(S; g(\cdot), Y), \text{ s.t. } \mathbb{E}[\ell(g(\cdot), Y)] \leq \epsilon. \quad (22)$$

Since $I_\alpha^A(S; \tilde{g}(\cdot), Y) \geq 0$ with equality if and only if $g(\cdot) \perp S|Y$, minimizing (10) with α -loss achieves EO. In practice, as the performance constraint ϵ in (22) increases, the FUR formulation in (22) will approach perfect EO of $g(\cdot)$ w.r.t. Y and S by enforcing $H_\alpha^A(S|g(S, X), Y) = H_\alpha^A(S|Y)$.

D. Alternate Minimax Algorithm

Algorithm 1 details the steps used to learn the FUR model in a data-driven manner.

Algorithm 1 Alternating minimax FUR algorithm

Input: dataset \mathcal{D} , distortion parameter D , # of decorrelator iterations T , # of adversary iterations J for each round of decorrelator update

Output: Optimal generative decorrelator parameter θ_p

procedure ALTERNATE MINIMAX(\mathcal{D}, D, T, J)

 Initialize decorrelator parameter θ_p^1 , adversary parameter θ_a^1 , and step size η_1

for $t = 1, \dots, T$ **do**

 Random minibatch of M datapoints $\{x_{(1)}, \dots, x_{(M)}\}$ drawn from full dataset

 Generate $\{\hat{x}_{(1)}, \dots, \hat{x}_{(M)}\}$ via $\hat{x}_{(i)} = g(x_{(i)}; \theta_p^t)$

 Apply update rule for step size η_t

 Set $\omega_a^1 = \theta_a^t$

for $j = 1, \dots, J$ **do**

 Update the adversary parameter θ_a^{t+1} by stochastic gradient ascent for epoch j

$$\omega_a^{j+1} = \omega_a^j + \eta_t \nabla_{\omega_a^j} \frac{1}{M} \sum_{i=1}^M -\ell(h(\hat{x}_{(i)}; \omega_a^j), s_{(i)}), \quad \eta_t > 0$$

 Set $\theta_a^{t+1} = \omega_a^{J+1}$

 Compute the descent direction $\nabla_{\theta_p^t} \ell(\theta_p^t, \theta_a^{t+1})$, where $\ell(\theta_p^t, \theta_a^{t+1})$ is defined in (23)

 Perform line search along $\nabla_{\theta_p^t} \ell(\theta_p^t, \theta_a^{t+1})$ and update

$$\theta_p^{t+1} = \theta_p^t - \eta_t \nabla_{\theta_p^t} \ell(\theta_p^t, \theta_a^{t+1})$$

return θ_p^{T+1}

To incorporate the distortion constraint into the learning algorithm, we use the *penalty method* [21] to replace the constrained optimization problem by a series of unconstrained

problems. Under the penalty method, the unconstrained optimization problem is formed by adding a penalty to the objective function. This penalty consists of a parameter ρ_t multiplied by a measure of violation of the constraint. Therefore, in Algorithm 1, the constrained optimization problem of the decorrelator can be approximated by a series of unconstrained optimization problems with the loss function

$$\begin{aligned} \ell(\theta_p^t, \theta_a^{t+1}) = & -\frac{1}{M} \sum_{i=1}^M \ell(h(g(x_{(i)}; \theta_p^t); \theta_a^{t+1}), s_{(i)}) \\ & + \rho_t (\max\{0, \frac{1}{M} \sum_{i=1}^M d(g(x_{(i)}; \theta_p^t), x_{(i)}) - D\})^2, \end{aligned} \quad (23)$$

where ρ_t is a penalty coefficient which increases with the number of iterations t . For convex optimization, the solution to the series of unconstrained problems will eventually converge to the solution of the original constrained problem [21].

E. Proof for Theorem 3

Since $\mathbb{E}_{X, \hat{X}}[d(\hat{X}, X)] = \mathbb{E}_{X, \hat{X}}[\|X - \hat{X}\|^2] = \mathbb{E}\|Z + \beta\|^2 = \|\beta\|^2 + \text{tr}(\Sigma_p)$, the distortion constraint implies that $\|\beta\|^2 + \text{tr}(\Sigma_p) \leq D$. Let us consider $\hat{X} = X + Z + \beta$, where $\beta \in \mathbb{R}$ and Σ_p is a diagonal covariance whose diagonal entries are given by $\{\sigma_{p_1}^2, \dots, \sigma_{p_m}^2\}$. Given the MAP adversary's optimal inference accuracy in (13), the objective of the decorrelator is

$$\min_{\beta, \Sigma_p} P_d^{(G)}, \text{ s.t. } \|\beta\|^2 + \text{tr}(\Sigma_p) \leq D. \quad (24)$$

Define $\frac{1}{\gamma} \ln \frac{1-q}{q} = \eta$. After some algebra, the gradient of $P_d^{(G)}$ w.r.t. γ is given by

$$\frac{\partial P_d^{(G)}}{\partial \gamma} = \frac{1}{2\sqrt{2\pi}} \left(qe^{-\frac{(\eta-\frac{\gamma}{2})^2}{2}} + (1-q)e^{-\frac{(\eta+\frac{\gamma}{2})^2}{2}} \right),$$

which is always positive. Thus, $P_d^{(G)}$ is monotonically increasing in γ . As a result, (24) is equivalent to

$$\begin{aligned} \min_{\beta, \sigma_{p_1}^2, \dots, \sigma_{p_m}^2} & \sum_{i=1}^m \frac{\mu_i^2}{\sigma_i^2 + \sigma_{p_i}^2}, \\ \text{s.t. } & \|\beta\|^2 + \text{tr}(\Sigma_p) \leq D \\ & \sigma_{p_i}^2 \geq 0 \quad \forall i \in \{1, 2, \dots, m\}. \end{aligned} \quad (25)$$

The optimization in (25) is analogous to the well-studied rate-distortion problem for independent Gaussian sources and the optimal solution given by reverse water-filling [36, Chap. 10.3.3]. Using similar techniques, we obtain $\sigma_{p_i}^{*2} = \max\{|\mu_i|/\sqrt{\lambda_0^*} - \sigma_i^2, 0\} = (|\mu_i|/\sqrt{\lambda_0^*} - \sigma_i^2)^+$ with $\sum_{i=1}^m \sigma_{p_i}^{*2} = D$ leading to the results in the theorem.

REFERENCES

- [1] H. F. Ladd, "Evidence on discrimination in mortgage lending," *Journal of Economic Perspectives*, vol. 12, no. 2, pp. 41–62, 1998.
- [2] D. Pedreshi, S. Ruggieri, and F. Turini, "Discrimination-aware data mining," in *14th ACM SIGKDD*, 2008, pp. 560–568.
- [3] C. Song and V. Shmatikov, "Overlearning reveals sensitive attributes," *arXiv:1905.11742*, 2019.
- [4] M. Feldman, S. A. Friedler, J. Moeller, C. Scheidegger, and S. Venkatasubramanian, "Certifying and removing disparate impact," in *21th ACM SIGKDD*, 2015, pp. 259–268.
- [5] C. Dwork, M. Hardt, T. Pitassi, O. Reingold, and R. Zemel, "Fairness through awareness," in *Proc. Innovations in Th. CS*, 2012, pp. 214–226.
- [6] F. Calmon, D. Wei, B. Vinzamuri, K. N. Ramamurthy, and K. R. Varshney, "Data pre-processing for discrimination prevention: Information-theoretic optimization and analysis," *IEEE JSAC*, vol. 12, no. 5, 2018.
- [7] M. Kearns, S. Neel, A. Roth, and Z. S. Wu, "Preventing fairness gerrymandering: Auditing and learning for subgroup fairness," in *Proc. Intl. Conf. Mach. Learning (ICML)*, 2018, pp. 2564–2572.
- [8] M. Hardt, E. Price, and N. Srebro, "Equality of opportunity in supervised learning," in *Proc. NeurIPS*, 2016, pp. 3315–3323.
- [9] A. Chouldechova, "Fair prediction with disparate impact: A study of bias in recidivism prediction instruments," *Big data*, vol. 5, no. 2, pp. 153–163, 2017.
- [10] B. H. Zhang, B. Lemoine, and M. Mitchell, "Mitigating unwanted biases with adversarial learning," *arXiv preprint arXiv:1801.07593*, 2018.
- [11] D. Madras, E. Creager, T. Pitassi, and R. Zemel, "Learning adversarially fair and transferable representations," *arXiv:1802.06309*, 2018.
- [12] H. Edwards and A. J. Storkey, "Censoring representations with an adversary," in *The 4th Intl. Conf. Learning Representations*, 2016.
- [13] F. Calmon, D. Wei, B. Vinzamuri, K. N. Ramamurthy, and K. R. Varshney, "Optimized pre-processing for discrimination prevention," in *NeurIPS*, 2017, pp. 3992–4001.
- [14] S. Hajian, J. Domingo-Ferrer, A. Monreale, D. Pedreschi, and F. Giannotti, "Discrimination-and privacy-aware patterns," *Data Mining and Knowledge Discovery*, vol. 29, no. 6, pp. 1733–1782, 2015.
- [15] J. Hamm, "Minimax filter: learning to preserve privacy from inference attacks," *J. Mach. Learn. Research*, vol. 18, no. 1, pp. 4704–4734, 2017.
- [16] C. Huang, P. Kairouz, X. Chen, L. Sankar, and R. Rajagopal, "Context-aware generative adversarial privacy," *Entropy*, vol. 19, no. 12, 2017.
- [17] A. Tripathy, Y. Wang, and P. Ishwar, "Privacy-preserving adversarial networks," *arXiv preprint arXiv:1712.07008*, 2017.
- [18] M. Bertran, N. Martinez, A. Papadaki, Q. Qiu, M. Rodrigues, G. Reeves, and G. Sapiro, "Adversarially learned representations for information obfuscation and inference," in *Proc. ICML*, 2019, pp. 614–623.
- [19] I. Goodfellow, J. Pouget-Abadie, M. Mirza, B. Xu, D. Warde-Farley, S. Ozair, A. Courville, and Y. Bengio, "Generative adversarial nets," in *Proc. NeurIPS*, 2014, pp. 2672–2680.
- [20] M. Mirza and S. Osindero, "Conditional generative adversarial nets," *arXiv preprint arXiv:1411.1784*, 2014.
- [21] W. E. Lillo, M. H. Loh, S. Hui, and S. H. Zak, "On solving constrained optimization problems with neural networks: A penalty method approach," *IEEE Trans. Neural Nets.*, vol. 4, no. 6, pp. 931–940, 1993.
- [22] Google, "Tensorflow constrained optimization (TFCO)," https://github.com/google-research/tensorflow_constrained_optimization/blob/master/README.md.
- [23] T. Sypherd, M. Diaz, J. K. Cava, G. Dasarathy, P. Kairouz, and L. Sankar, "A tunable loss function for robust classification: Calibration, landscape, and generalization," *arXiv preprint:1906.02314*, 2021.
- [24] D. McNamara, C. S. Ong, and R. C. Williamson, "Costs and benefits of fair representation learning," in *Proc. AAAI/ACM Conference on AI, Ethics, and Society*, 2019.
- [25] A. A. Alemi, I. Fischer, J. V. Dillon, and K. Murphy, "Deep variational information bottleneck," *arXiv preprint arXiv:1612.00410*, 2016.
- [26] E. Creager, D. Madras, J.-H. Jacobsen, M. Weis, K. Swersky, T. Pitassi, and R. Zemel, "Flexibly fair representation learning by disentanglement," in *Proc. ICML*, vol. 97, 2019, pp. 1436–1445.
- [27] J. Liao, O. Kosut, L. Sankar, and F. P. Calmon, "Privacy under hard distortion constraints," *arXiv preprint arXiv:1806.00063*, 2018.
- [28] S. Asoodeh, M. Diaz, F. Alajaji, and T. Linder, "Estimation efficiency under privacy constraints," *IEEE Trans. Inform. Th.*, vol. 65, no. 3, 2018.
- [29] P. Kairouz, J. Liao, C. Huang, and L. Sankar, "Censored and fair universal representations using generative adversarial models," https://github.com/LalithaSankarResearch/CFUR_source-code.
- [30] M. Abadi, A. Agarwal, P. Barham, E. Brevdo, Z. Chen, C. Citro, G. S. Corrado, A. Davis, J. Dean, M. Devin *et al.*, "Tensorflow: Large-scale machine learning on heterogeneous distributed systems," *arXiv preprint arXiv:1603.04467*, 2016.
- [31] D. P. Kingma and J. Ba, "Adam: A method for stochastic optimization," *arXiv preprint:1412.6980*, 2017.
- [32] R. Kohavi, "Scaling up the accuracy of naive-bayes classifiers: A decision-tree hybrid," in *KDD*, vol. 96, 1996, pp. 202–207.
- [33] Z. Zhang, Y. Song, and H. Qi, "Age progression/regression by conditional adversarial autoencoder," in *IEEE CVPR*, 2017.
- [34] T. Nguyen and S. Sanner, "Algorithms for direct 0–1 loss optimization in binary classification," in *Proc. ICML*, 2013, pp. 1085–1093.
- [35] S. Verdú, " α -mutual information," in *Inform. Th. Apps Workshop*, 2015.
- [36] T. M. Cover and J. A. Thomas, *Elements of information theory*. John Wiley & Sons, 2012.